

doi: 10.3788/gzxb20144307.0710001

基于独立成分分析的遥感影像可匹配性度量

巨西诺, 郭文普, 孙继银, 李琳琳, 伍明

(第二炮兵工程大学, 西安, 710025)

摘 要: 为了提高景象匹配中基准图制备的效率和可靠性, 对遥感影像图源的可匹配性进行分析, 提出一种基于独立成分分析的遥感影像可匹配性度量方法. 利用独立成分分析提取纹理基函数, 并计算其概率分布, 确定可匹配区域; 然后定义可匹配区域所占面积比例指标、离散性指标和稳定性指标; 最后, 利用三个指标构建遥感影像可匹配性度量模型. 实验表明, 该遥感影像可匹配性指标与实际匹配概率相关性强, 提高了基准图制备的可靠性, 能够满足景象匹配图源筛选的实际需求.

关键词: 图像匹配; 图像质量; 独立成分分析; 遥感; 基准图制备; 导弹制导; 可匹配性

中图分类号: TP391

文献标识码: A

文章编号: 1004-4213(2014)07-0710001-7

Remote Sensing Image Matching Performance Metric Based on Independent Component Analysis

JU Xi-nuo, GUO Wen-pu, SUN Ji-yin, LI Lin-lin, WU Ming

(The Second Artillery College, Xi'an 710025, China)

Abstract: To improve the reliability of reference map preparation for scene matching, it is necessary to analyze the matching performance of remote sensing image. Remote sensing image matching performance metric was proposed based on independent component analysis. Firstly, texture basis functions are produced based on independent component analysis and a set of probability functions that describe the coefficients distribution corresponding to each of the texture basis functions are calculated to extract matching regions. Secondly, the area ratio index, distribution index and stability index for matching regions are defined. Lastly, remote sensing image matching performance metric is constructed based on the three indexes. The experiment shows that the proposed remote sensing image matching performance metric index is highly correlated to real matching probability. It improves the reliability of reference map preparation and can meet the need of remote sensing images selection for scene matching.

Key words: Image matching; Image quality; Independent component analysis; Remote sensing; Reference map preparation; Missile guidance; Matching performance

OCIS Codes: 100.2960; 100.3008; 100.3000

0 Introduction

Due to the high precision, self-contained, low energy consumption, small size and other prominent properties, downward looking scene matching guidance has become one of the key technologies in compound guidance weapon system. The guidance accuracy of missile weapon system is directly affected by the

reliability of reference maps. In practical application, reference maps are mainly extracted from appropriate regions of remote sensing images selected by specific rules and translated into data information for guidance system through image correcting and feature extraction. The reliability of reference map is closely related to quality of remote sensing image, and it is a difficult problem for currently battling security

Foundation item: The National Defense Pre-study Foundation of China (No. 5132202XX)

First author: JU Xi-nuo(1986-), female, Ph. D. candidate, mainly focuses on image process and scene matching. Email: jxnwawj@163.com

Supervisor: SUN Ji-yin(1952-), male, professor, Ph. D. degree, mainly focuses on image process and automated command. Email: Sunjiyin@163.com

Received: Oct. 16, 2013; **Accepted:** Jan. 21, 2014

<http://www.photon.ac.cn>

department to select images suitable for preparing reference maps from large numbers of remote sensing images. Currently, the remote sensing image selection mainly relies on manual interpretation. It not only requires a high level of knowledge for the staff but also has low efficiency and reliability. The reference maps can't meet the actual demand which results in tremendous waste of resources. Different with traditional image quality assessment, remote sensing image quality evaluation for scene matching mainly estimates image matching performance, which is not only related to imaging quality, but also to the matching performance of corresponding regions. The computational complexity of matching simulation experiments for large remote sensing images is high and can't meet the actual demand. A simple and quick method for remote sensing images matching performance metric is avidly needed.

Normalized Product (NProd) correlation algorithm is a commonly matching algorithm for scene matching and many high adaptive matching algorithms are designed based on NProd^[1]. The matching precision of NProd algorithm is mainly affected by the complexity of gray feature and the number of similar regions. The traditional reference map preparation methods include image variance, gray entropy, edge density, independent pixel number, correlation peak feature, repetitive spatial patterns, self-matching probability and so on^[2-6]. Among them, image variance, gray entropy, edge density and independent pixel number mainly analyze the complexity of gray feature, and correlation peak feature, repetitive spatial patterns and self-matching probability analyze the region similarity. The former methods only consider one-dimensional statistical features of gray without considering the structure feature of image, and it results in unreliable extraction region. The latter rules require large numbers of correlation matching experiments on the basis of abundant image samples extracted from large remote sensing image and can't meet the demand of real-time.

The salience and uniqueness of different regions in remote sensing image is calculated to analyze the matching performance. Remote sensing image matching performance metric is proposed based on Independent Component Analysis (ICA)^[7-9]. Firstly, texture basis functions are calculated based on FastICA algorithm^[10-12] in training samples extracted from remote sensing images, matching regions are extracted using the salience, and uniqueness of image computed by the coefficient distribution of texture basis

functions. Secondly, matching area ratio, distribution and stability are calculated. Finally, remote sensing image matching performance metric model is built using regression method.

1 Texture basis function extraction

1.1 Independent component analysis

ICA is a blind signal separation method developing in recent years, which decomposes the observed mixed signal into mutually statistically independent signals. Assume that there are an n-dimensional unknown source signal $\mathbf{S} = [s_1, \dots, s_n]^T$ and an m-dimensional observed signal $\mathbf{X} = [x_1, \dots, x_m]^T$. \mathbf{X} is a weighted combination matrix decomposed as follows

$$\mathbf{X} = \mathbf{A}\mathbf{S} \quad (1)$$

where $\mathbf{A} \in \mathbf{R}^{m \times n}$ is mixed matrix and the vectors of \mathbf{S} are mutually statistically independent. The goal of ICA is to find separation matrix \mathbf{W} . An n-dimensional mutually statistically independent output vector $\mathbf{Y} = [y_1, \dots, y_n]^T$ is produced through transforming \mathbf{X} using \mathbf{W} to approximate the source signal.

$$\mathbf{Y} = \mathbf{W}\mathbf{X} \quad (2)$$

1.2 Texture basis function extraction based on FastICA

For the ICA model $\mathbf{X} = \mathbf{A}\mathbf{S}$, if the observed signal \mathbf{X} is a group of image signals, \mathbf{A} can be called as texture basis function which is basic elements of image, and $\mathbf{S} = [s_1, \dots, s_n]^T$ is the weighted coefficient for image reconstruction based on texture basis functions. Then, image can be defined as linear weighted texture basis functions, which is shown in Fig. 1.

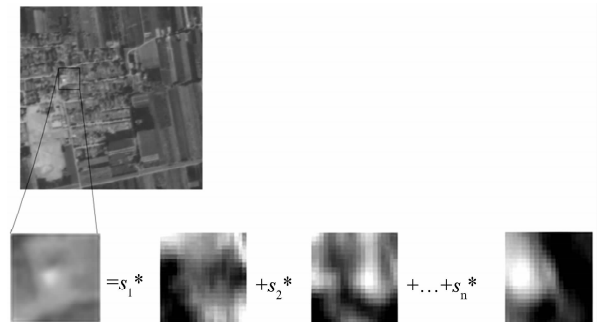


Fig. 1 Image decomposing

FastICA is a fast ICA algorithm based on non-Gaussian maximization principle to approximate negative entropy as the objective function, and the non-Gaussian maximum of $\mathbf{W}\mathbf{X}$ is found using fixed-point iteration. 5000 image blocks with size of 33×33 defined as training samples are randomly extracted from 20 remote sensing images. The training samples are translated into one-dimensional data with size of 1089×1 to constitute a training data set \mathbf{X} with size of 1089×5000 . 50 texture basis functions extracted using FastICA for the experiment are shown in Fig. 2.

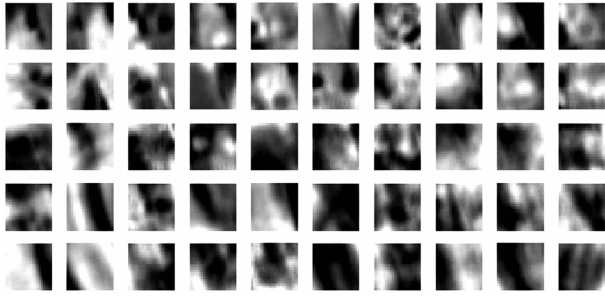


Fig. 2 Texture basic function

2 Remote sensing image matching performance metric

2.1 Remote sensing image matching region extraction

The probability of target image can be expressed by separate component. Then, the probability of image $\mathbf{X}=\mathbf{AS}$ can be expressed as

$$P(\mathbf{X})=P(\mathbf{AS})=\frac{P(\mathbf{S})}{|\det(\mathbf{A})|} \quad (3)$$

If texture basis function \mathbf{A} is fixed value, the probability distribution of Gaussian random variables can be converted to the product of one-dimensional random variables probability distribution due to \mathbf{S} is statistically independent^[13]. It is shown as Fig. (4).

$$P(\mathbf{X})=\frac{P(\mathbf{S})}{|\det(\mathbf{A})|}\propto P(\mathbf{S})=\prod_{k=1}^n P(s_k) \quad (4)$$

Fig (4) shows that the probability of the target image \mathbf{X} in the whole image only depends on coefficients \mathbf{S} calculated by \mathbf{W} .

The main goal for remote sensing image matching performance metric is to analyze the uniqueness and salience of target image. Uniqueness aims at false detection rate, while salience is for image feature reliability. Image is composed of different texture basis functions. There will be less similar image blocks which means stronger uniqueness if the probability of texture basis functions coefficient is smaller. Image uniqueness matrix \mathbf{U} can be defined by the probability of texture basis functions coefficient

$$\mathbf{U}(i,j)=-\frac{\sum_{k=1}^n \log(P(s_k))}{n}-\min_{k=1,\dots,n}(\log(P(s_k))) \quad (5)$$

(i,j) is coordinate of image block center.

Logical matrix \mathbf{U}_L is calculated with given threshold computed using the method proposed in Ref. [14]. In \mathbf{U}_L , matching region is named as 1 and no matching region is named as 0.

2.2 The reliability of matching region

Generally, the larger the area ratio of matching region in remote sensing image is, the greater the matching performance is. However, the distribution and stability of matching region greatly affect remote sensing image matching performance. The area ratio based on the uniqueness can't accurately predict

matching performance without considering the reliability of matching region. Analysis of area ratio, distribution and stability of matching region is needed for remote sensing image matching performance metric.

2.2.1 Matching region area ratio index

Matching region area ratio index A is defined as

$$A=\frac{\sum_{i=1}^m \sum_{j=1}^n \mathbf{U}_L(i,j)}{m \times n} \quad (6)$$

where $m \times n$ is the size of image block.

2.2.2 Matching region distribution index

Remote sensing image matching region distribution index D is calculated as follows

Step1: Logical matrix \mathbf{U}_L is divided into 16 sub-blocks with same size;

Step2: Calculated $\text{num}_k, k=1, \dots, 16$, which is the number of "1" for each sub-block;

Step3: Calculate the mean and standard deviation std of the array num_k and matching region distribution index D is defined as;

$$D=\frac{\text{std}+\text{mean}}{m \times n} \quad (7)$$

where $m \times n$ is the size of image block.

2.2.3 Matching region stability index

Feature stability can be described by edge density of matching region. The larger the edge density is, the more the image information is and the better the matching performance is. Canny operator with anti-noise, good adaptability can extract ideal edge and is used for edge extraction in this paper. Matching region stability index S is defined as:

$$S=\frac{\text{edge}}{m \times n} \quad (8)$$

where edge means the number of edge pixels, and $m \times n$ is the size of image block. A large number of experiments show that the correlation between feature stability index and real matching probability is good when the low-pass and high-pass threshold of Canny operator is defined as $[0, 2 \ 0, 4]$.

2.3 Remote sensing image matching performance metric

The larger the remote sensing image matching region area ratio is, the more suitable for route planning and reference map preparation. The probability of randomly selecting good real-time image will be higher if the matching region distribution is highly dispersive. Two remote sensing images with size of 2560×2560 is chose to analyze the relationship between matching probability and area ratio index A , distribution index D , stability index S . Simulation is a primary measure to analyze performance of matching algorithm due to high price of flight experiments. The remote sensing image is equally divided into 100 sub-

images and matching probability is calculated using simulation. Area ratio index A , distribution index D , and stability index S are calculated using the proposed method. Fig. 3 shows the relationship between

matching probability and area ratio index A , distribution index D , stability index S for the two remote sensing images, while many outliers exist and the correlation is poor. Therefore, remote sensing

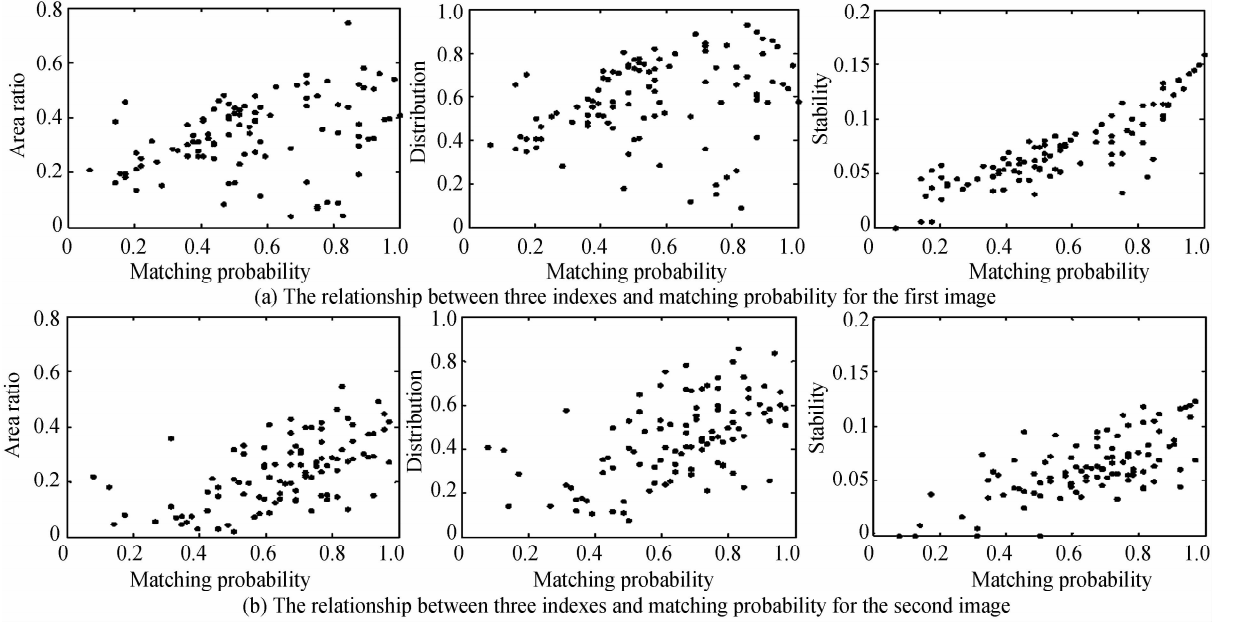


Fig. 3 The relationship between three indexes and matching probability

image matching performance metric model is built based on area ratio index A weighted by distribution index D and stability index S . The model is shown as

$$IQA = e^{\lambda D + \beta S} \cdot A + \gamma \quad (9)$$

λ , β and γ are adjustment factors. The correlation between IQA and real matching probability is great when $\lambda = -2.16$, $\beta = 13.58$, $\gamma = 0.37$ calculated using regression analysis with a large number of samples.

Forest, farmland and other vegetation information take a large proportion in remote sensing image, which are usually not suitable for reference map preparation due to low gray variation, high repetition and lack of salient target. Standard deviation is used to choose primary matching region of remote sensing image to improve the efficiency. In order to reduce influence of gray correction, image enhancement and other subsequent processing for standard deviation, dynamic threshold is used for image filtering. A large number of experiments show that the image filtering works best when the standard deviation threshold is defined as the 4/5 of the whole image standard deviation. Remote sensing image is quite large and must be divided into sub-block, referring to the size of the reference map in the actual application. Uniqueness is calculated in sub-block and the size of texture basis function is the same as the size of real-time image. It is insignificant for uniqueness when the sub-block is greater than the

reference map. Fig. 4 shows the process of remote sensing image matching performance metric.

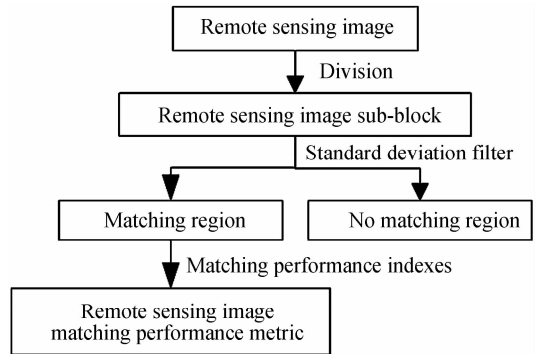


Fig. 4 Remote sensing image matching performance metric process

3 Experiment and analysis

In order to verify the validity of the index, two SPOT satellite images and an ALOS satellite image shown in Fig. 5 are selected for simulation experiment. The sizes of images are 5120×5120 , 2560×2560 , 1024×640 and the sizes of sub-blocks are 512×512 , 256×256 and 128×128 in turn. Matching probability based on NProd algorithm is calculated through simulation experiment^[15]. Fig. 6 shows the relationship between IQA and matching probability.

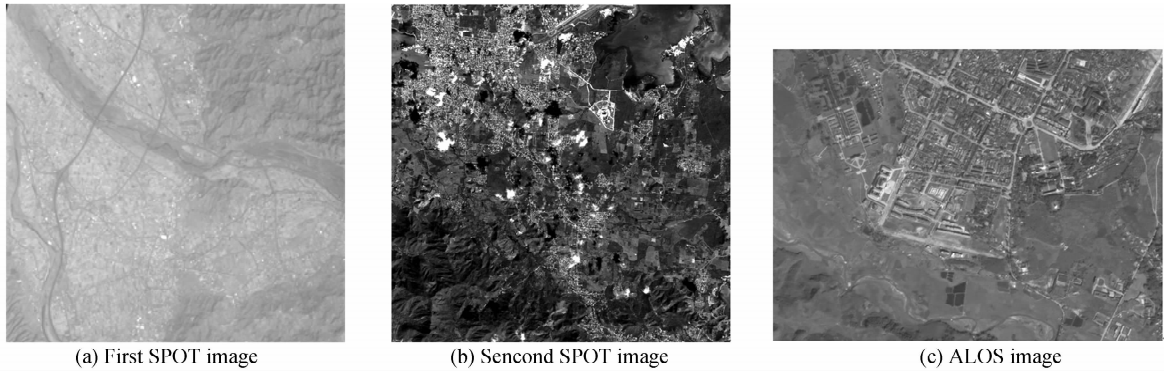


Fig. 5 Three remote sensing images

Fig. 6 shows that matching probability is more than 0.6 when the corresponding *IQA* index is greater than 0.6, and matching probability is more than 0.8 when the corresponding *IQA* index is greater than 0.8. Most of the data is consistent with the actual situation, but there are some outliers. It is caused mainly by two

aspects. On the one hand, simulation is high complexity and uncertainty; on the other hand, in order to improve the versatility of the model, the large difference of training images leads to low accuracy of model.

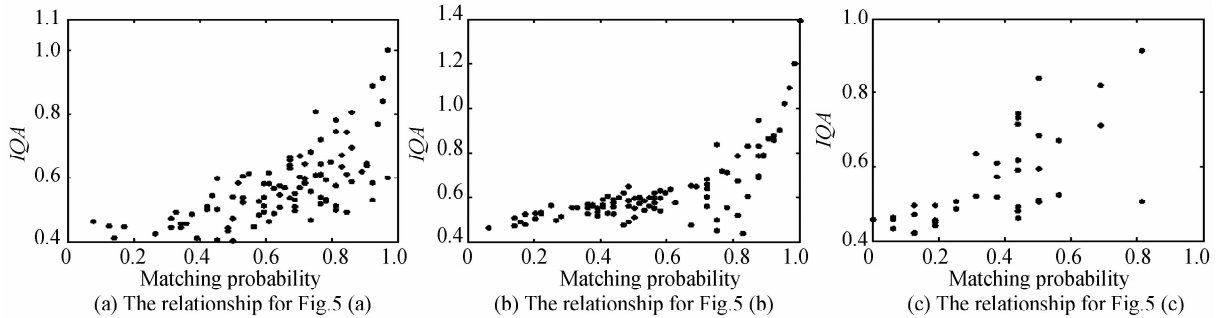


Fig. 6 The relationship between *IQA* and matching probability

There are two ways to solve this problem; 1) matching performance metric model can be trained separately using several sub-blocks extracted from each remote sensing image; 2) gray correction can be used

to reduce the degree of differences of remote sensing images. Matching performance metric model can be trained using corrected images. Fig. 7 shows the results of the two improved methods.

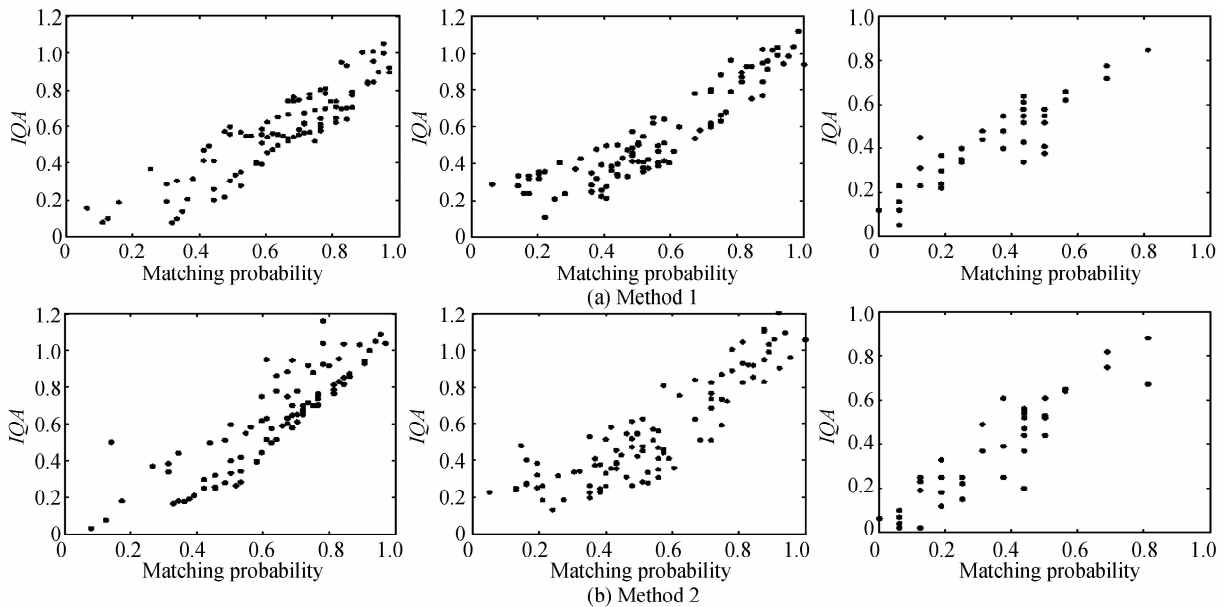


Fig. 7 The relationship between *IQA* and matching probability based on improved model for Fig. 5 (a)~(c)

As can be seen from Fig. 7, the correlation of resulting data using method 1 is stronger than method 2. But the method 1 is required to train model for each image and computational complexity is high. Relatively speaking, method 2 is very simple. Typically, the size of original remote sensing image is more than $10\,000 \times 10\,000$. It is very difficult for direct simulation. The proposed index can quickly evaluate the matching performance of image. A remote sensing image with size of $15\,207 \times 13\,771$ is chosen to test the practical application. The size of sub-block is 512×512 and we get 524 sub-blocks after preliminary screening. Matching performance is evaluated using, proposed method 1 and method 2 by simulation. In method 1, 100 sub-blocks are selected to train the model. The results are shown in Fig. 8.

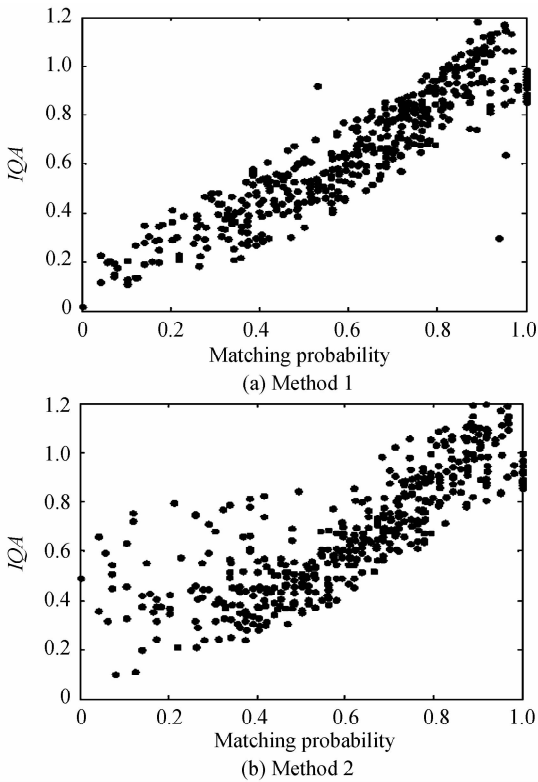


Fig. 8 Matching performance metric using different methods

The time-consuming is 7 126. 7 seconds, 528. 7 seconds and 1 982. 4 seconds separately in same conditions. Fig. 8 shows that the outliers of method 2 is more than method 1, but the number is within a controllable range. In practical applications, we can use different methods based on actual demand.

The index can predict the remote sensing image matching performance. For scene matching, it is only need to select the remote sensing images suitable for reference map generation. It can be transformed into a classification problem, i. e. matching region, uncertain matching region, no matching region. Due to the

characteristics of *IQA* index, classification mode is shown as Fig. (10).

$$\begin{cases} \text{if } IQA < 0.6, \text{image} \in \text{NMR} \\ \text{if } 0.6 \leq IQA < 0.8, \text{image} \in \text{DMR} \\ \text{if } IQA \geq 0.8, \text{image} \in \text{MR} \end{cases} \quad (10)$$

NMR, DMR and MR denote no matching region, uncertain matching region and matching region separately. If image belongs to matching region, it means it can be used for reference map preparation and NProd matching algorithm is feasible. When it belongs to no matching region, it can't generate reference map. If image belongs to uncertain matching region, the greater *IQA* is, the higher the probability of belonging to matching region is. NProd matching algorithm is unsuitable and the matching performance requires further analysis.

Compare the reliability of reference map preparation based on traditional methods and proposed method. Fig. 5 (b) is selected for reference map preparation with size of 256×256 and the size of real-time image is 32×32 . Traversing step is 128. The first reference map set is generated using traditional methods such as information entropy, variance, independent pixel number, self-matching probability and repetitive spatial patterns. The threshold for every index is experiential threshold. The second reference map set is selected in matching region computed by the proposed index. The third reference map set is selected from matching region using traditional methods. Matching probability based on NProd matching algorithm is computed using simulation experiment for three reference map sets. The result is shown in Tabel 1.

Table 1 Matching performance assessment for reference maps

Reference map	1 st set	2 nd set	3 rd set
Number of total reference maps	156	129	115
Number of invalid reference maps	37	13	1
Average matching probability	78.66%	90.62%	96.18%

If matching probability is less than 85%, the reference maps are invalid. Tabel 1 shows that the ratio of invalid reference maps based on traditional methods is high and average matching probability is low. It can't meet the actual demand. While matching probability of reference map set based on proposed index is high. On the basis of the combination of traditional methods and the proposed method, the average matching probability is larger than 95%. It can meet the needs of scene matching. Besides, traditional methods such as repetitive spatial patterns and self-

matching probability are time-consuming due to extensive traversal operation and not suitable for reference map source selection. Analysis of proposed algorithm shows that the maximization of time complexity for matching region extraction is $O(G \cdot H)$, where G is the number of image pixels and H is the size of the texture basis function, when the texture basis function is fixed value. The time-consuming is much lower than traditional simulation experiment. It can meet the actual demand.

4 Conclusion

In order to improve the reliability of reference image preparation, remote sensing image source must be pre-screened, that of remote sensing image matching performance metric. Calculating the uniqueness and salience of different regions in remote sensing image using ICA. Matching region is chose and remote sensing image matching performance metric index is defined based on area ratio index, distribution index and stability index. Experiments show that the proposed index is highly associated with actual matching probability. The proposed index can classify remote sensing images accurately and improves efficiency and reliability of reference map preparation. It can meet the needs of practical application.

References

- [1] YANG Xiao-gang. On location approach and simulation technology of multi-source image matching for missile[D]. Xi'an: The Second Artillery College, 2006.
- [2] CAO Fei, YANG Xiao-gang, MIU Dong, *et al.* Study on reference image selection roles for scene matching guidance[J]. *Application Research of Computers*, 2005, (5): 137-139.
- [3] YANG Xiao-gang, CAO Fei, HUANG Xian-xiang, *et al.* Reference image preparation approach for scene matching simulation[J]. *Journal of System Simulation*, 2010, **22**(4): 850-852.
- [4] FU Meng-yin, ZHANG Xiao-chen. Reference map generation techniques for scene matching guidance: an overview [C]. Proceedings of the 29th Chinese Control Conference, 2010, 2805-2809.
- [5] ZHANG Xiao-chen, FU Meng-yin. Selection method for scene matching area based on information entropy [J]. *Systems Engineering and Electronic*, 2011, **33**(5): 1089-1093.
- [6] YANG Zhao-hui, CHEN Ying-ying. Support vector machine for scene matching area selection [J]. *Journal of Tongji University (Natural Science)*, 2009, **37**(5): 690-695.
- [7] HYVARINEN A. Independent component analysis [M]. ZHOU Zong-tan transl. Beijing, Publishing House of Electronics Industry, 2007.
- [8] LI Xi, CHEN Xue-hong, CHEN Xiao-ling, *et al.* Blind unmixing of hyperspectral mixed pixels assisted by wavelet packet decomposition [J]. *Acta Photonica Sinica*, 2011, **40**(6): 835-842.
- [9] LUO Yuan, WANG Ling-xue, JIN Wei-qi. Independent component analysis and its application to image processing [J]. *Optical Technique*, 2012, **38**(5): 520-527.
- [10] NIAN Yong-jian, ZHANG Zhi, WANG Li-bao, *et al.* Target segmentation for hyperspectral imagery based on FastICA [J]. *Acta Photonica Sinica*, 2010, **39**(6): 1003-1009.
- [11] ZHANG Da-bao, SHAO Hong. Improved FastICA algorithm based on symmetric orthogonalization [C]. IEEE International Conference on Signal Processing (ICSP), 2012, 1:75-78.
- [12] DERMOUNE A, WEI T. FastICA algorithm: five criteria for the optimal choice of the nonlinearity function [J]. *Signal Processing*, 2013, **61**(8): 2078-2087.
- [13] LOU Tian-tian. Visual saliency based on natural scene statistics [D]. Shanghai: East China Normal University, 2011.
- [14] GE Tao. A method for image salient regions detection based on layers and dynamic threshold [D]. Beijing: Beijing Jiaotong University, 2006.
- [15] YANG Xiao-gang, ZUO Sen, HUANG Xian-xiang, *et al.* Integral experiment and simulation system for image matching [J]. *Journal of System Simulation*, 2010, **22**(6): 1360-1364.